FULL WAVE ANALYSIS OF EDGE-GUIDED MODE MICROSTRIP ISOLATOR

Tarief F. Elshafiey, James T. Aberle and El-Badawy El-Sharawy

Telecommunications Research Center
Arizona State University, Tempe AZ 85287-7206

Abstract

This paper presents a full-wave analysis of three Edge-Guided Mode microstrip isolator structures. Galerkin's technique in the spectral domain is used to calculate the insertion loss and the isolation of the structures. The paper presents figures of merit of different multilayer structures. A multilayer structure resulted in increased isolation and lower insertion loss.

1 Introduction

The isolator is one of the most widely used magnetic devices. The principle of operation of these devices is based on the field displacement effect; i.e the microwave field configurations of the forward and backward propagating waves are different. If an absorbing resistive film is placed at one edge of the conductor , then different attenuation of these two waves occurs and an isolator is realized. The geometry of an isolator with a resistive thin film is shown in Fig. 1. Experimental work on this type of isolator has been widely reported in the literature [1] -[6]. However, no full-wave analysis of the present structure has been reported to date.

2 Full Wave Formulation

A versatile technique for formulating the Green's function for structures with transversely magnetized ferrite substrates was first described by El-Sharawy [7]. This technique utilizes the transmission matrix of the ferrite layer, wherein all the fields are expressed in terms of arbitrary constants that arise in the solution of the wave equation of the medium. The same technique is used here to derive the Green's function for structures containing a normally magnetized ferrite substrate. The

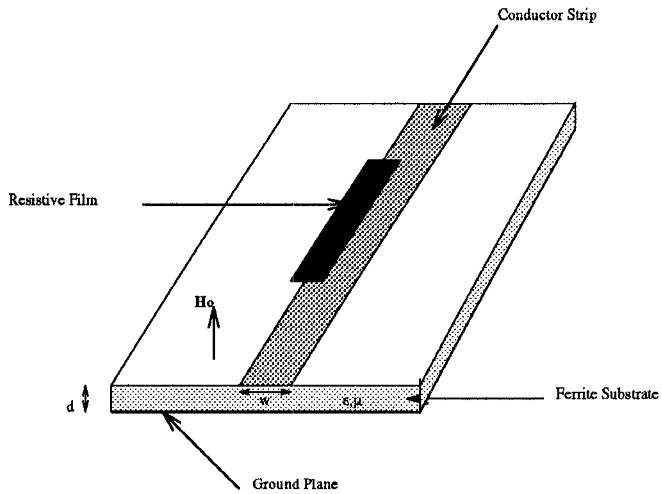

Figure 1: Edge-Guided isolator with resistive film loading.

transmission matrix $\tilde{\bar{\bar{T}}}$ is a 4×4 matrix written as [7]

$$\begin{bmatrix} \tilde{\bar{E}}_2 \\ \tilde{\bar{J}}_2 \end{bmatrix} = \tilde{\bar{\bar{T}}} \begin{bmatrix} \tilde{\bar{E}}_1 \\ \tilde{\bar{J}}_1 \end{bmatrix} = \begin{bmatrix} \tilde{\bar{\bar{T}}}^E & \tilde{\bar{\bar{Z}}}^T \\ \tilde{\bar{\bar{Y}}}^T & \tilde{\bar{\bar{T}}}^J \end{bmatrix} \begin{bmatrix} \tilde{\bar{E}}_1 \\ \tilde{\bar{J}}_1 \end{bmatrix} \quad (1)$$

where $\tilde{\bar{\bar{T}}}^E$, $\tilde{\bar{\bar{Z}}}^T$, $\tilde{\bar{\bar{Y}}}^T$, $\tilde{\bar{\bar{T}}}^J$ are 2×2 submatrices of $\tilde{\bar{\bar{T}}}$, "$\sim$" denotes the spatial Fourier transform defined as

$$\tilde{\bar{E}}(K_x, K_y) = \int_{-\infty}^{\infty} \int_{-\infty}^{\infty} \bar{E}(x, y) e^{-jK_x x} e^{-jK_y y} \, dx \, dy \quad (2)$$

$\tilde{\bar{E}}_1$ and $\tilde{\bar{E}}_2$ are the tangential electric field at the boundaries of the layer, and $\tilde{\bar{J}}_1$ and $\tilde{\bar{J}}_2$ are the tangential surface currents defined by $\tilde{\bar{J}}_n = \hat{z} \times \tilde{\bar{H}}_n$, where $\tilde{\bar{H}}_n$ is the tangential magnetic field at the nth surface of the layer.

Because of the nature of the problem, the normally biased ferrite substrate transmission matrix is more difficult to derive than the one for transversely biased ferrite. The derivation was greatly facilitated by the use of the symbolic computation software, MAPLE V.

We investigated three different isolator structures. The first structure comprises a single normally magnetized ferrite substrate as shown in Fig. 2. In the second structure, we added another dielectric layer underneath the ferrite layer as shown in Fig. 3. The third structure, called "drop-in element", is an isolator structure compatible with Monolithic Microwave Integrated Circuits (MMIC). In this structure, a dielectric substrate with relative permittivity equal to 9.8 is used. To form an EG isolator, we place a piece of ferrite with a resistive thin film on top of the dielectric as shown in Fig. 4.

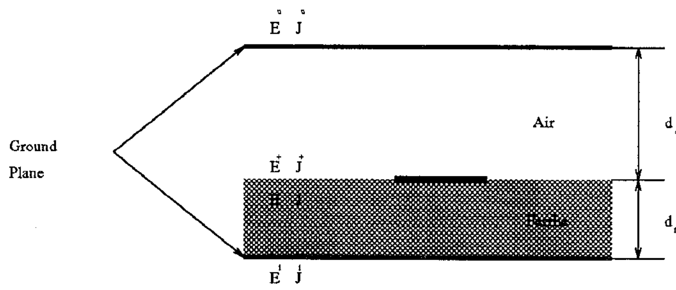

Figure 2: Geometry of single layer structure.

2.1 Green's Function Formulation

A spectral-domain Green's function, $\tilde{\bar{\bar{G}}}$, is formulated that relates the transformed electric field $\tilde{\bar{E}}_s$ on one surface to the transformed electric surface currents $\tilde{\bar{J}}_s$, on the same surface. This relation has the form,

$$\tilde{\bar{E}}_s(k_x, k_y) = \tilde{\bar{\bar{G}}}(k_x, k_y)\tilde{\bar{J}}_s(k_x, k_y) \quad (3)$$

Using the transmission matrix, Green's functions can be formulated in the spectral domain for single and multi-layer structures. For the single-layer structure, the Green's function is

$$\tilde{\bar{\bar{G}}} = (\tilde{\bar{\bar{Z}}}_f^T \tilde{\bar{\bar{T}}}_f^{J^{-1}} + \tilde{\bar{\bar{G}}}_a^{-1})^{-1} \quad (4)$$

where $\tilde{\bar{\bar{Z}}}_f^T$ and $\tilde{\bar{\bar{T}}}_f^J$ are submatrices of the transmission matrix of a normally biased ferrite layer and $\tilde{\bar{\bar{G}}}_a$ is a semispace Green's function, which is calculated by taking the limit of the dielectric Green's function when the thicknes of the layer, d_d, goes to infinity and the dielectric constant goes to one.

$$\tilde{\bar{\bar{G}}}_a = \lim_{\substack{d_d \to \infty \\ \epsilon_d \to 1}} \tilde{\bar{\bar{G}}}_d \quad (5)$$

where $\tilde{\bar{\bar{G}}}_d$ is formed using the dielectric transmission matrix derived by El-Sharawy [7].

For the ferrite-dielectric structure, the Green's function is

$$\tilde{\bar{\bar{G}}} = (\tilde{\bar{\bar{Z}}}^T \tilde{\bar{\bar{T}}}^{J^{-1}} + \tilde{\bar{\bar{G}}}_a^{-1})^{-1} \quad (6)$$

and $\tilde{\bar{\bar{Z}}}^T$ and $\tilde{\bar{\bar{T}}}^J$ are the elements of $[T_{new}]$, where

$$[\tilde{T}_{new}] = [\tilde{T}_f][\tilde{T}_d]$$

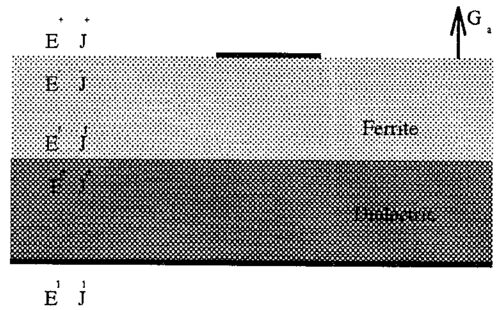

Figure 3: Geometry of double layer structure.

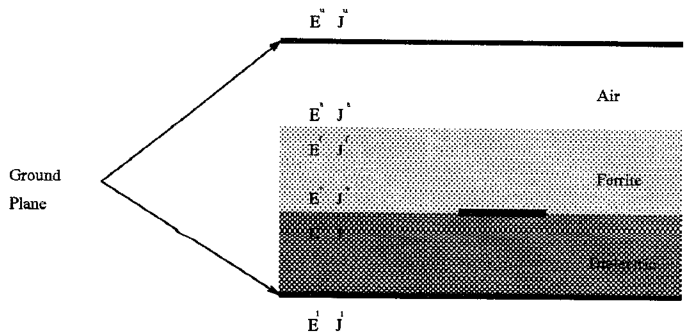

Figure 4: Geometry of drop-in element structure.

which is the result of the ferrite and dielectric transmission matrix multiplication.

For the three layer structure (the drop-in element) the Green's function is

$$\overline{\overline{\tilde{G}}}= (\overline{\overline{Z}}_u^T \overline{\overline{T}}_u^{J^{-1}} + \overline{\overline{Z}}_d^T \overline{\overline{T}}_d^{J^{-1}})^{-1} \tag{7}$$

where $\overline{\overline{Z}}_u^T$ and $\overline{\overline{T}}_u^J$ are the elements of the new transmission matrix which resulted from the ferrite and air transmission matrix multiplication.

3 Numerical Results and Conclusion

We compared our Green's function for the single layer structure shown in Fig. 2 with the Green's function derived by Pozar [8] using the boundary condition method. An excellent agreement between these two methods was achieved.

Since the Green's function of a multi-layer structure including a normally ferrite substrate is not available in the literature, we compared the limiting case of the ferrite with the Green's function derived by Aberle for multi-layer dielectric structures [9]. Again excellent agreement was achieved.

We constructed a 2-D MoM code for simulating an EG mode isolator with resistive loading as shown in Fig. 1. First, we examined the limiting case of ferrite with zero ferrite parameters, which is essentially the dielectric case, and compared our results to the widely published results for dielectric microstrip. The phase constants for forward and backward waves are shown in Fig. 5. The computed insertion loss and isolation are given in Fig. 6

A preliminary analysis of the three isolator structures indicates that the best electrical performance is given by the double-layer structure shown in Fig. 3. While, the performance of the triple-layer structure shown in Fig. 4 is not as good as the other two structures, its advantage is that it can be compatible with MMIC. The insertion loss of the three isolator structures is compared in Fig. 7 and the isolation of the three structures is compared in Fig. 8.

For a single layer of ferrite isolator, the field ellipticities at the upper and the lower boundaries with air counteract each other. If the air at one of these boundaries is replaced by a dielectric layer, as in Figures 4 and 3, one of the counteracting ellipticities is replaced by a co-acting ellipticity which leads to increase in the nonreciprocity and the isolation as well [10]-[12].

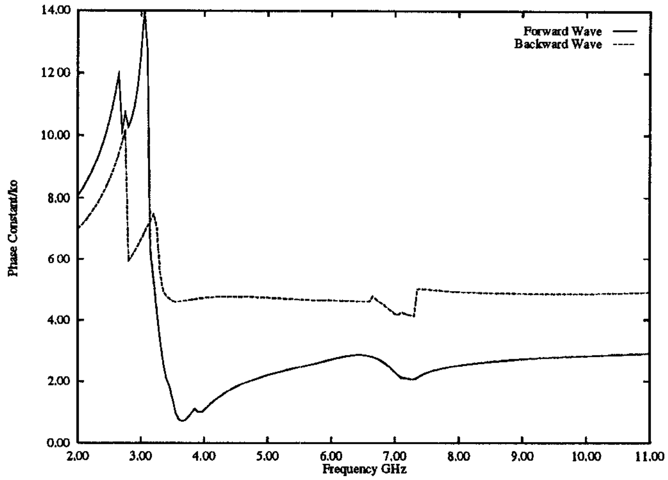

Figure 5: The phase constants of forward and backward waves $d = 7.62 \times 10^{-4}m$, $\epsilon_f = 12.0$, $4\pi M_s = 1750G$, $H_{dc} = 800Oe$, $\Delta H = 80.Oe$, $R_s = 100\Omega$, $W = 1.016 \times 10^{-2}m$.

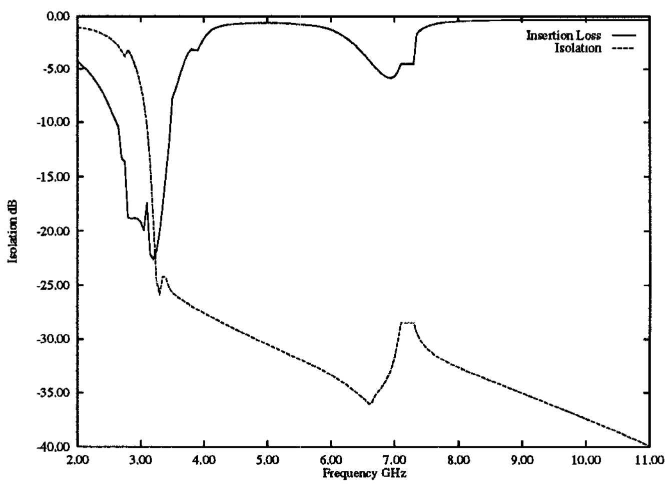

Figure 6: Computed isolation and insertion loss $d = 7.62 \times 10^{-4}m$, $\epsilon_f = 12.0$, $4\pi M_s = 1750G$, $H_{dc} = 800Oe$, $\Delta H = 80.Oe$, $R_s = 100\Omega$, $W = 1.016 \times 10^{-2}m$

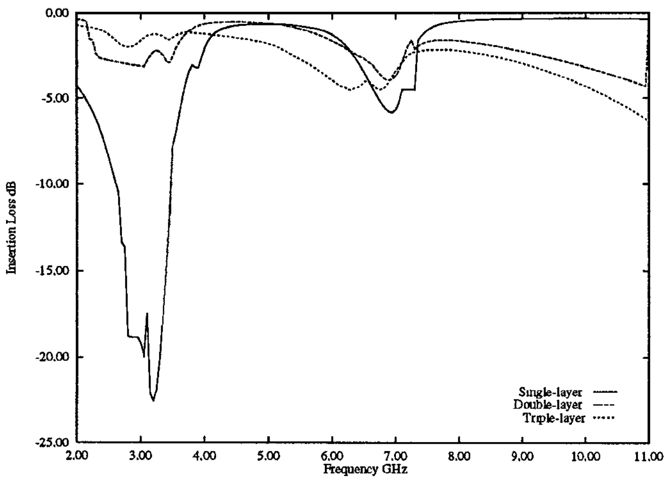

Figure 7: Comparison of the insertion loss for three isolator structures. ($4\pi M_s = 1750$ G, $H_{dc} = 800$ Oe, $\Delta H = 80.$ Oe, $R_s = 100\Omega$, $W = 1.016E-2$ m. For the single-layer: $d_f = 7.62E-04$ m, $\epsilon_f = 12.0$. For the double-layer: $d_d = 2.62E-04$ m, $\epsilon_d = 3.00$. For the triple-layer: $d_d = 4.00E-04$ m, $\epsilon_d = 8.90$ $d_a = 5.00E-03$ m, $\epsilon_a = 1.00$).

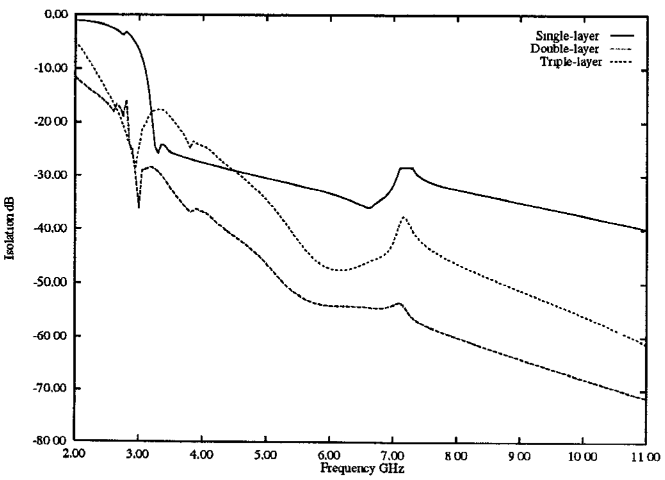

Figure 8: Comparison of the isolation for three isolator structures. The same parameters are as in Fig. 7

References

[1] M. E. Hines, "Reciprocal and nonreciprocal modes of propagation in ferrite stripline and microstrip devices," *IEEE Trans. Microwave Theory Tech.*, vol. MTT-19, pp. 442–451, May 1971.

[2] G. T. Roome and H. A. Hair, "Thin ferrite devices for microwave integrated circuits," *IEEE Trans. Microwave Theory Tech.*, vol. MTT-16, pp. 411–420, July 1968.

[3] K. Araki, T. Koyama, and Y. Naito, "Reflection problem in a ferrite stripline," *IEEE Trans. Microwave Theory Tech.*, vol. MTT-24, pp. 491–498, Aug. 1976.

[4] M. Dydyk, "One path to wideband isolator design (part i)," *Microwaves*, vol. 16(1), pp. 54–58, Jan. 1977.

[5] M. Dydyk, "One path to wideband isolator design (part ii)," *Microwaves*, vol. 16(2), pp. 50–56, Feb. 1977.

[6] R. C. Kane and T. Wong, "An edge-guided mode microstrip isolator with transverse slot discontinuity," in *IEEE MTT-S Digest*, pp. 1007–1010, 1990.

[7] E. El-Sharawy and R. W. Jackson, "Coplanar waveguide and slot line on magnetic substrates: Analysis and experiment," *IEEE Trans. Microwave Theory Tech.*, vol. MTT-36, pp. 1071–1079, June 1988.

[8] D. M. Pozar, "Radiation and scattering characteristics of microstrip antennas on normally biased ferrite substrates," *IEEE Trans. Antennas Propagat.*, vol. AP-40, pp. 1084–1092, Sep. 1992.

[9] J. T. Aberle, D. M. Pozar, and J. Manges, "Phased arrays of probe-fed stacked microstrip patches," *IEEE Trans. Antennas Propagat.*, vol. AP-42, pp. 920–927, July 1994.

[10] E. El-Sharawy, *Full Wave Analysis of Printed Lines on Magnetic Substrates*. PhD thesis, University of Massachusetts, 1989.

[11] G. Bock, "New multilayered slot-line structures with high nonreciprocity," *Electronics Letters*, vol. 19, pp. 966–968, Nov. 1983.

[12] T. I. M. Geshiro, "Analysis of double-layered finlines containing a magnetized ferrite," *IEEE MTT Symp.*, vol. MTT-S 87, pp. 743–744, June 1987.